

Echelle gratings tiling method based on lateral shearing interferometry

Yifan Li^{a,b}, Xiaotao Mi^{a,*}, Xiangdong Qi^a, Shanwen Zhang^a, Guojun Yang^a, Hongzhu Yu^a, Xiaotian Li^a, Wenhao Li^a

^a Changchun Institute of Optics, Fine Mechanics and Physics, Chinese Academy of Sciences, Changchun, Jilin 130033, China

^b University of Chinese Academy of Sciences, Beijing 100049, China

ARTICLE INFO

Keywords:

Echelle grating
Tiled gratings
Shearing interferometry

ABSTRACT

A method for echelle gratings tiling based on lateral shearing interferometry is proposed. Fringe patterns of the grating assembly are generated by a wedge plate. Mosaic errors can be calculated and corrected by observing the working order and its adjacent order. An experimental mosaic of two 50 mm × 50 mm, 79 grooves/mm echelles is aligned to verify the theory. The rms wavefront is better than 0.04 wavelength. Angular and translation sensitivities of less than 1 arcsec and 10 nm are achieved respectively.

1. Introduction

Diffraction gratings play an essential role in many modern technical fields. Areas like chirped-pulse amplification (CPA) systems and astronomical spectroscopic telescope systems require large-aperture gratings [1,2]. However, direct manufacture of large gratings could encounter technical difficulties. A mosaic grating composed of well-aligned small-aperture gratings is a technically possible and financially acceptable alternative. In the last three decades, there has been a growing number of publications referring to mosaic gratings. Some early research [3–5] mainly focused on optical designs for pulse compressors. Harimoto [6] calculated the far-field pattern distribution of an array grating and set up an alignment tolerance criterion, proving the possibility of aligning gratings based on far-field intensity distribution. Qiao et al. [7] addressed that the aberrations in large-size far-field imaging systems could lead to deviations in measured wavefronts. In this case, the final criterion for tiling quality should be near-field wavefront. A thorough analysis of the interferometry method and its implementation for the assembly of three 0.47 m × 0.47 m gratings was presented. Zeng et al. [8] used a two-color heterodyne interferometer, which can separate two different phase errors by wavelength, and improve measurement accuracy by employing a heterodyne scheme. But this work did not consider adjusting angular errors. Sharma et al. [9] combined the two methods by simultaneously monitoring far-field profiles and interferograms. This combination can easily differentiate mismatches because the two methods are sensitive to different mosaic errors.

A method for tiling gratings often involves two steps [10]. Firstly the

0th order diffraction beam is utilized to keep gratings co-planar, then in-plane errors are processed by measuring a different (usually the 1st) diffraction order. This approach might not be as effective when applied to echelle gratings, for the energy of a beam diffracted from the 0th order of a low-frequency echelle grating may not be enough for interferometric measurement. The mosaic in ESPRESSO [11] used finely ground spacers to equalize the height of the gratings, therefore in-plane errors can be assessed by observing interferograms of the working order and adjacent orders. While there was no requirement for strict alignment of phase shifts, this procedure itself was not very convenient. Cong et al. [12] modified the gratings by coating a small region with aluminum alongside the grooves on the surface. So when the incident beam transmits along the grating normal, a reflection beam will function as the 0th order diffraction, enabling regular measurements by interferometry. The limitation is that the gratings need to be customized, and it is uncertain whether the special structure will introduce stray light or other issues that will affect the performance of the grating assembly in practical applications.

In this paper, we present a method for echelle grating tiling based on lateral shearing interferometry. The shearing interferogram of a two-grating assembly can be divided into three regions. The fringe pattern in the middle region is related to mosaic errors. The other two regions contain reference fringes. All errors can be distinguished and calculated by analyzing patterns of two different diffraction orders. We present a theoretical analysis of the method as well as simulations of the fringe patterns. An experimental platform was established to verify the theory. Two 50 mm × 50 mm echelle gratings with 79 grooves/mm were

* Corresponding author.

E-mail address: mixiaotao@ciomp.ac.cn (X. Mi).

<https://doi.org/10.1016/j.optlastec.2021.107475>

Received 16 April 2021; Received in revised form 20 August 2021; Accepted 23 August 2021

Available online 28 August 2021

0030-3992/© 2021 Elsevier Ltd. All rights reserved.

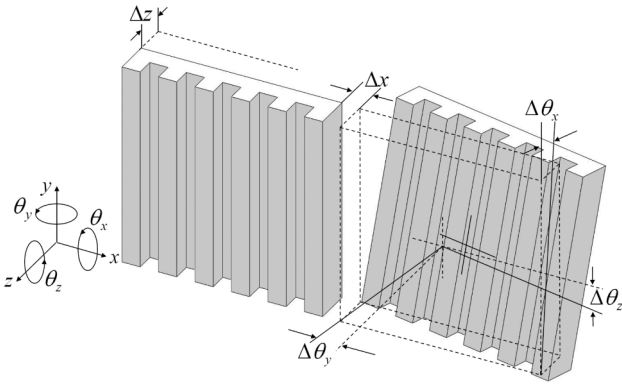


Fig. 1. Demonstration of grating mosaic errors.

mosaicked by a customized mechanism. Additional measurement errors and accuracy tests will be discussed at the end.

2. Theoretical analysis

2.1. Grating mosaic alignment errors and wavefront phase analysis

There are six degrees of freedoms between two adjacent gratings [13]. As shown in Fig. 1, the six alignment errors can be categorized into shifts along axes (Δx , Δy , Δz) and rotations around axes ($\Delta\theta_x$, $\Delta\theta_y$, $\Delta\theta_z$). Shift parallel with grooves (Δy) can be considered having no effects on wavefront qualities in a small range. The other five errors will cause deviations of the diffraction wavefront and require adjustments. Since the gap between two gratings (Δx) is physically impossible to eliminate, we define a perfect mosaic as $\Delta z = 0$, $\Delta\theta_x = 0$, $\Delta\theta_y = 0$, $\Delta z = 0$, and $\Delta x = nd$, where d is the grating period and n is an integer. A perfect mosaic should have the same optical performance as a single large grating of the same size. Besides, mismatch of grating periods (Δd) will also lead to wavefront inconsistency. Considering that the gratings used for the mosaic are supposed to be replicas of a high-quality echelle master, we assume them to be identical in the following discussions. The wavefront of a two-grating mosaic can now be expressed as [14]:

$$\frac{d\phi}{dx} = \frac{2\pi}{\lambda} \frac{(\cos\alpha + \cos\beta)}{\cos\beta} \Delta\theta_y \quad (1a)$$

$$\frac{d\phi}{dy} = -\frac{2\pi}{\lambda} [(\cos\alpha + \cos\beta)\Delta\theta_x + (\sin\alpha + \sin\beta)\Delta\theta_z] \quad (1b)$$

$$\phi_z = \frac{2\pi}{\lambda} [(\sin\alpha + \sin\beta)\Delta x - (\cos\alpha + \cos\beta)\Delta z] \quad (1c)$$

where λ is the wavelength, α is the incident angle, β is the diffraction angle, m is the diffraction order, ϕ_z is the piston phase error, $d\phi/dx$ and $d\phi/dy$ represent the transverse phase gradients in the beam. The perfect mosaic condition can be expressed as $d\phi/dx = 0$, $d\phi/dy = 0$, $\phi_z = 2n\pi$. Eq. (1) shows that mosaic errors have various effects on the wavefront. While $\Delta\theta_y$ is individual, $\Delta\theta_x$ and $\Delta\theta_z$ as well as Δx and Δz are compensation pairs. This means one single wavefront measurement cannot separate all mosaic errors, a compensated phase would be acquired instead. Therefore an additional measurement is required to remove all errors, with at least one parameter changed among wavelength, incident angle, and diffraction order [15].

The grating equation can be expressed as:

$$\sin\alpha + \sin\beta = \frac{m\lambda}{d} \quad (2)$$

Eq. (1) can be rewritten as:

$$\frac{d\phi}{dx} = \frac{2\pi}{\lambda} \frac{(\cos\alpha + \cos\beta)}{\cos\beta} \Delta\theta_y \quad (3a)$$

$$\frac{d\phi}{dy} = -\frac{2\pi}{\lambda} [(\cos\alpha + \cos\beta)\Delta\theta_x + \frac{m\lambda}{d} \Delta\theta_z] \quad (3b)$$

$$\phi_z = \frac{2\pi m\lambda}{\lambda} \Delta x - (\cos\alpha + \cos\beta)\Delta z \quad (3c)$$

When the 0th order wavefront is measured, $\Delta\theta_z$ and Δx are irrelevant to phase differences. Therefore $\Delta\theta_y$, $\Delta\theta_x$ and Δz can be differentiated and calculated. Removing these three alignment errors is similar to mosaicking reflection mirrors, which will keep two gratings co-planar. Another measurement carried out in a diffraction order (usually the 1st order) will determine the value of $\Delta\theta_z$ and Δx . Grooves can be matched after adjusting these two in-plane errors, and a perfect mosaic status could be reached theoretically. This approach, despite being popular, may not be as effective when applied to echelle gratings. Echelles gratings typically blaze in high angles and are generally used in high orders. The energy of a 0th order diffraction beam may not be enough for interferometric measurements. Measurements should be carried out in the working order to achieve better results. At least two measurements are needed to provide enough equations to calculate all the errors mathematically. As we addressed above, the second measurement also requires that at least one of the three parameters is

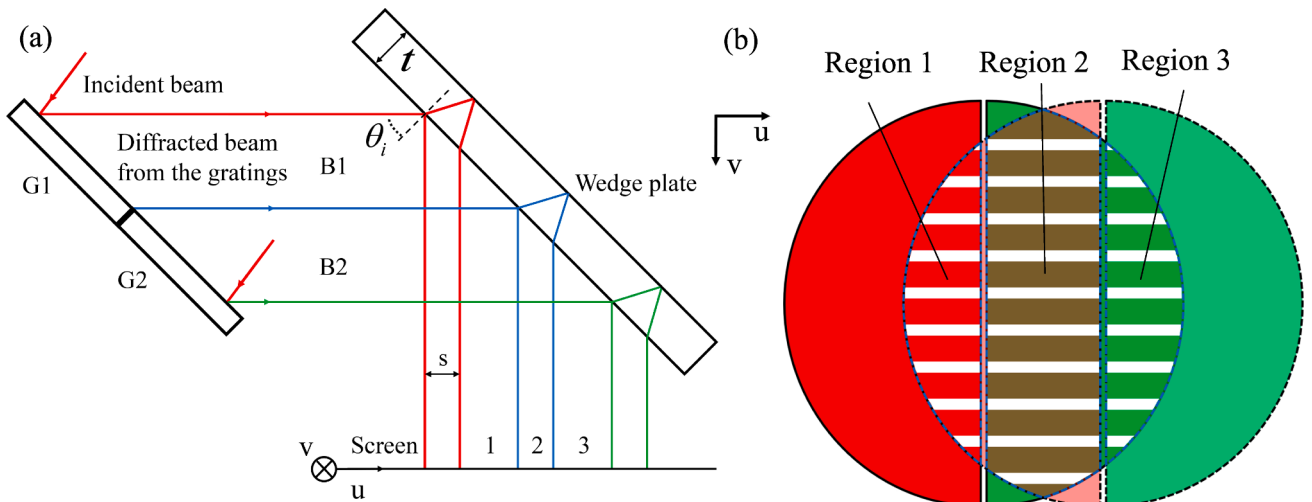


Fig. 2. (a) Schematic of dual-beam LSI, (b) Interference fringe pattern of dual-beam LSI.

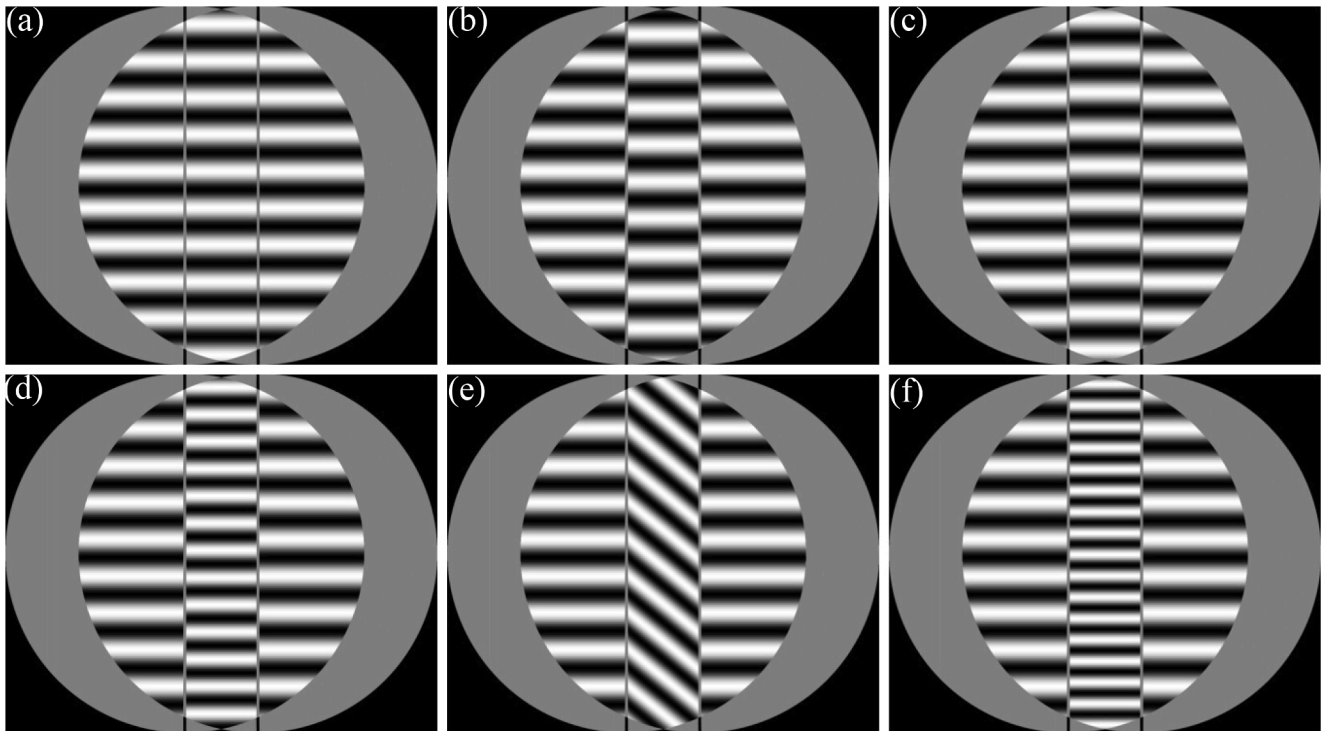


Fig. 3. Simulated interferograms (a) no errors, (b) $\Delta x = 100$ nm, (c) $\Delta z = 100$ nm, (d) $\Delta\theta_x = 50$ μ rad, (e) $\Delta\theta_y = 50$ μ rad, (f) $\Delta\theta_z = 50$ μ rad.

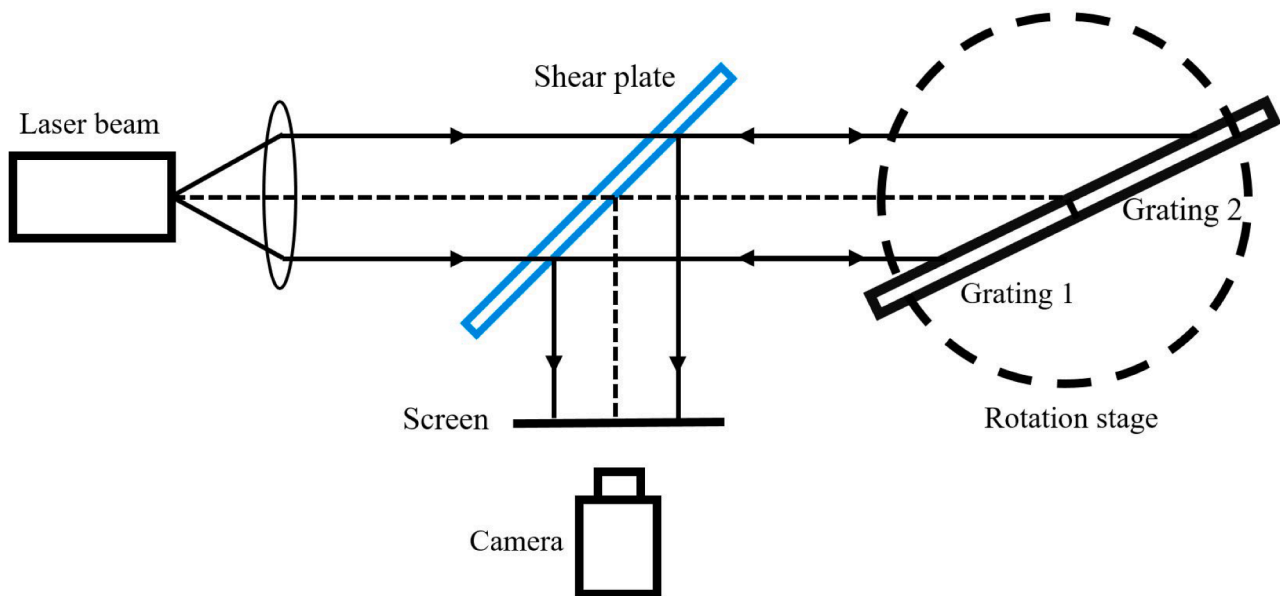


Fig. 4. Experiment setup of the tiling system.

different from the first one. However, the procedure is still flawed if only the wavelength of the beam or the incident angle is changed. When the phase we observed shows errors removed, which means $\phi_z = 2n\pi$, and we assume $\Delta z = 0$, according to Eq.(3c), Δx is not necessarily equal to an integer multiple of d , it is actually nd/m . This means when $|m| \geq 2$, Eq.(3c) would have two solutions at least. The gratings will not be aligned as expected if the adjustment value of Δx is false. Therefore, the second measurement must be taken in a different diffraction order, and the greatest common divisor of the two orders should be 1. Obviously, adjacent orders of the working order are convenient for operating.

2.2. Lateral shearing interferometry for mosaic errors measurement

Lateral shearing interferometry (LSI) is widely used for wavefront characterization. A wedged plate LSI has a simple configuration and does not need a reference beam, so it is not sensitive to environmental vibration. Reconstruction of the phase is relatively more complicated, for the LSI does not directly measure the phase, but rather its slope in the direction of the lateral shear. Normally it will take two interferograms in perpendicular directions to retrieve the wavefront. However, the unaligned grating mosaic is not a consistent surface but two separated ones. Some recent researches [16,17] have proved that a dual-beam phase can be processed with a single LSI interferogram. Fig. 2 shows

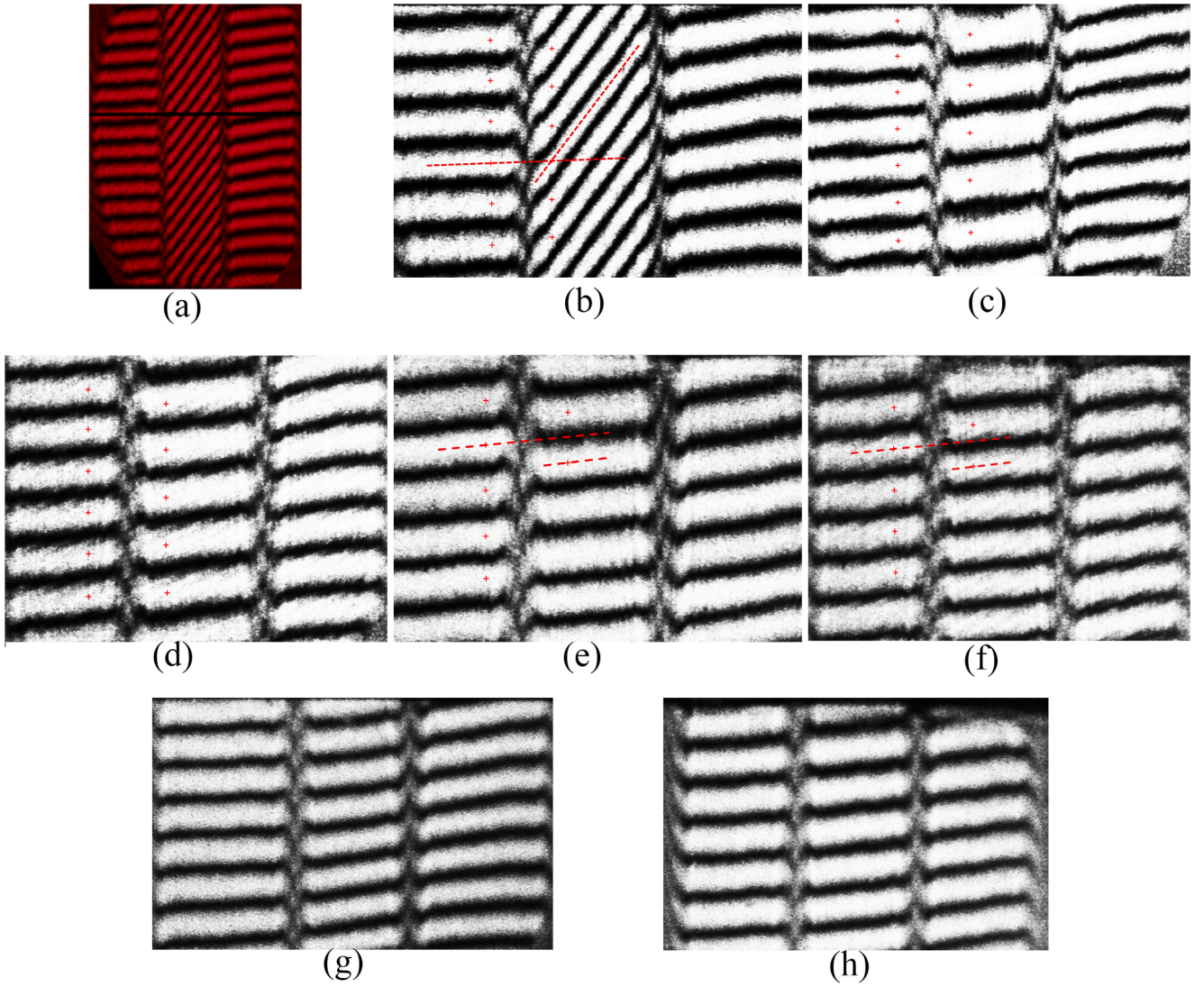


Fig. 5. Demonstration of tiling procedure (a) raw picture captured by camera, (b) chosen regions of interest, fringe slope measured (c) & (d) $\Delta\theta_y$ removed, fringe spacing of the -36th and -37th order measured, (e) & (f) $\Delta\theta_x$ and $\Delta\theta_z$ removed, phase shifts of the -36th and -37th order measured, (g) & (h) all errors eliminated, fringe patterns of the -36th and -37th order.

the principle of LSI for dual-beam. Take n and t as the refraction index and thickness of the glass. Two beams B1 and B2 originated from the gratings are adjacent to each other, with the incident angle of θ_i . The dual-beam will reflect on both the front and back surface of the plate, creating a shearing distance of s . The wedge angle θ_w is perpendicular to the shearing direction, introducing an angle θ_t between two reflected beams to generate fringes [18]. Therefore we have:

$$s = t \frac{\sin 2\theta_i}{\sqrt{n^2 - \sin^2 \theta_i}} \quad (4)$$

$$\theta_t = 2\theta_w \sqrt{n^2 - \sin^2 \theta_i} \quad (5)$$

Fig. 2(b) shows the interference fringe pattern on the screen. The fringes can be divided into three regions. In region 1 and region 3, reflection beams of B1 and B2 from the front surface of the plate interfere with their duplicates from the back surface. In region 2, the back surface reflection of B1 interferes with the front surface reflection of B2. We define region 1 as reference fringes, with fringe spacing $l_r = \lambda/\theta_t$. Fringe patterns in region 2 can be expressed as:

$$\Delta\Phi(u, v) = \frac{2\pi}{\lambda} [(\cos\alpha + \cos\beta) \frac{\Delta\theta_y}{\cos\beta} u - \Delta\theta_x v - \Delta z] + (\sin\alpha + \sin\beta)(\Delta x - \Delta\theta_z v) - \theta_t v] \quad (6)$$

Fringe spacing in u and v direction and phase shift can be derived as:

$$v_p = -\frac{\lambda}{(\cos\alpha + \cos\beta)\Delta\theta_x + (\sin\alpha + \sin\beta)\Delta\theta_z - \theta_t} \quad (7a)$$

$$u_p = \frac{\lambda \cos\beta}{(\cos\alpha + \cos\beta)\Delta\theta_y} \quad (7b)$$

$$\Delta\phi = \frac{2\pi}{\lambda} [(\sin\alpha + \sin\beta)\Delta x - (\cos\alpha + \cos\beta)\Delta z] \quad (7c)$$

Fringe spacing in the u direction can be acquired more conveniently by measuring the fringe slope. The fringe slope k_s can be written as:

$$k_s = \frac{v_p}{u_p} = -\frac{\Delta\theta_y (\cos\alpha + \cos\beta) \sec\beta}{(\cos\alpha + \cos\beta)\Delta\theta_x + (\sin\alpha + \sin\beta)\Delta\theta_z - \theta_t} \quad (8)$$

There are five unknown variables in Eq. (7)–(8). By measuring two different diffraction orders, we can get two sets of data to establish

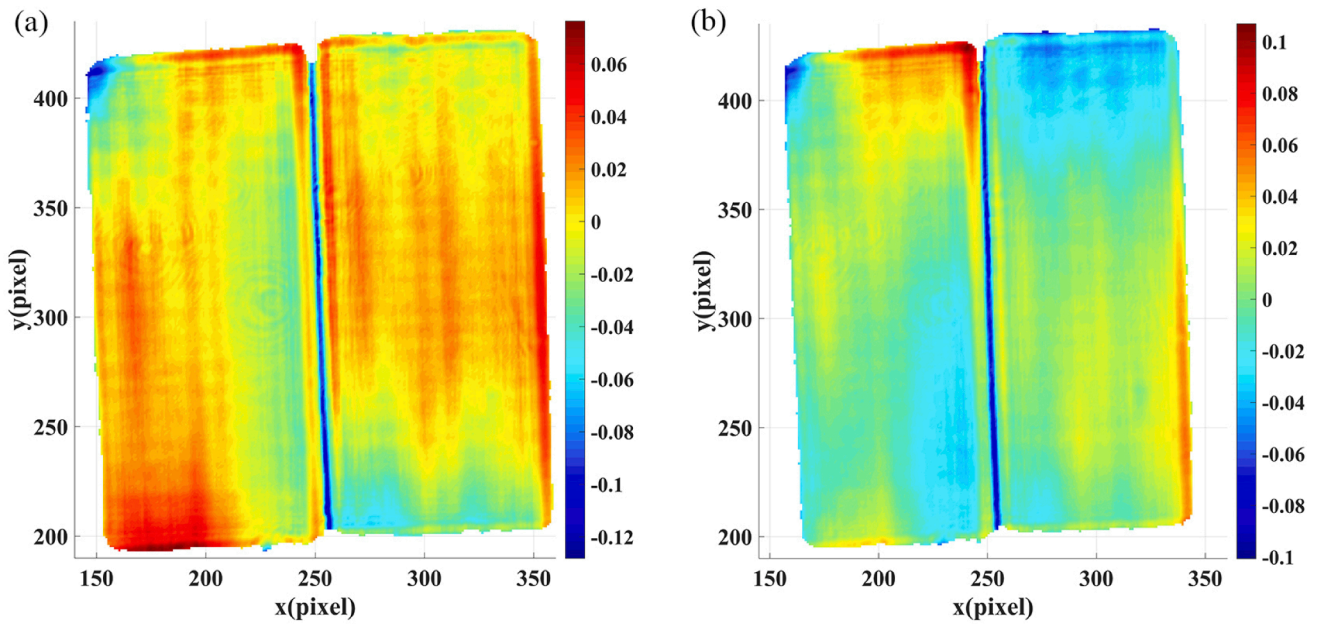


Fig. 6. Wavefront maps measured by Fizeau interferometer (wavelength = 632.8 nm). Color scale represents the wavefront value (λ). (a) wavefront of the -36 th order, rms 0.031λ , (b) wavefront of the -37 th order, rms 0.033λ .

simultaneous equations, therefore all errors can be solved.

3. Simulated interferograms of mosaic errors

Parameters similar to the actual experiment are used to generate interferograms. The incident beam is an ideal plane wave ($\lambda = 632.8$ nm). The grating assembly has two echelle gratings with 79 grooves/mm. Littrow configuration is used on -36 th order (incident angle = 64.137 deg.). The diffraction beam will then transmit to the wedge plate at an incident angle of 45 degree. The thickness, wedge angle, and refractive index of the wedge plate are 13 mm, 10 arcsec, and 1.457 respectively. Simulated interferograms are shown in Fig. 3. Reflected beams from the plate are both circle areas with a 50 mm diameter. Shearing distance is 10.2 mm in the u direction, and fringes appear in the overlap area. The interference area can be divided into three regions. We assume the left half of a circle represents the reference grating, and the right half represents the moving grating, and there is a gap of 2 mm between two gratings. Fig. 3(a) shows the ideal condition with no mosaic errors, the fringes in three regions are continuous and parallel to the u axis. Patterns in the middle region will change when errors exist. Fig. 3(b-f) are conditions with different types of errors. Δx and z will cause phase shifts along v axis, $\Delta\theta_x$ and z will change the fringe spacing, and $\Delta\theta_y$ will rotate the fringes.

4. Experiments and results analysis

4.1. Echelle gratings tiling experiment

The experiment was carried out on two 50 mm \times 50 mm, 79 grooves/mm echelle gratings. The most direct way is to measure two diffraction orders at the same time. This will require two independent interferometry systems, and the optical path would need to be extended to at least 1500 mm to prevent cross interfere of different orders. Our alternative solution was to put the assembly on a rotation stage to measure two orders separately. Fig. 4 shows the experimental setup. A laser beam of 100 mm diameter (wavelength 632.8 nm) was used as the light source. Two gratings were mounted on a customized mechanism. Two PZTs (PI 622.1) control piston shifting in two directions, and other three pico-motors controls three rotation-dimensions. The beam went through the

shear plate (Thorlabs SI500, thickness 13 mm, refractive index 1.457, wedge angle 16.2 arcsec by testing), diffracted by gratings, then returned to the plate. A scattering screen was placed perpendicular to the sheared beams to receive the fringes. Regions of interest were cropped from raw pictures, enhanced, marked, and further processed by computer programs.

First, we put a reflection mirror on the mosaic mechanism to determine the zero point of rotation stage. The ratio of image pixels to actual length was also calculated. Then two gratings were installed at Littrow angle of the -36 th order (64.137 deg.). Fig. 5 shows the fringe pattern in each step of the alignment procedure. Fringe spacing in region 1 & 2 and slope in region 2 were measured to calculate $\Delta\theta_y$ using Eq. (7a), (7b) and Eq. (8). Corresponding pico-motors were then driven to remove $\Delta\theta_y$. Next, fringe spacing in region 2 was measured again. The grating assembly was then rotated to the Littrow angle of the -37 th order (67.644 deg.) to do another measurement. Therefore $\Delta\theta_x$ and $\Delta\theta_z$ could be calculated using Eq. (7a). Similarly, $\Delta\theta_x$ and $\Delta\theta_z$ could be calculated using Eq. (7c) with phase shifts measured from two orders. The practical alignment progress involved multiple rounds of adjustments before a fine mosaic status was achieved. Fig. 5(g)&(h) show the fringe patterns of both orders after all errors were consider removed.

We did an independent test with a commercial Fizeau interferometer (Zygo GPI) to crosscheck the wavefront quality of the two orders. The grating assembly was considered as a single echelle. Therefore a regular surface testing procedure was conducted. The reshaped wavefront maps are displayed in Fig. 6. Results indicate that mosaic status of our grating assembly reached our expectation. The peak-to-valley variation of the wavefronts are less than 0.3λ , rms wavefronts are better than 0.04λ , and Strehl ratios are above 0.96 in both orders.

4.2. Mosaic accuracy analysis

Extra tests were conducted to verify the accuracy of the method. The grating assembly was pre-aligned before each test. Then one certain kind of error was deliberately introduced by equal steps. For angular tests each mechanical input step would add $\Delta\theta_x$, $\Delta\theta_y$ and $\Delta\theta_z$ by $0.3 \mu\text{rad}$, $0.462 \mu\text{rad}$ and $0.429 \mu\text{rad}$ respectively. Each time we added 10 steps to θ_x and θ_y and 5 steps to θ_z axis into make the changes of fringe patterns distinguishable. Fig. 7 shows results from one of the multiple tests.

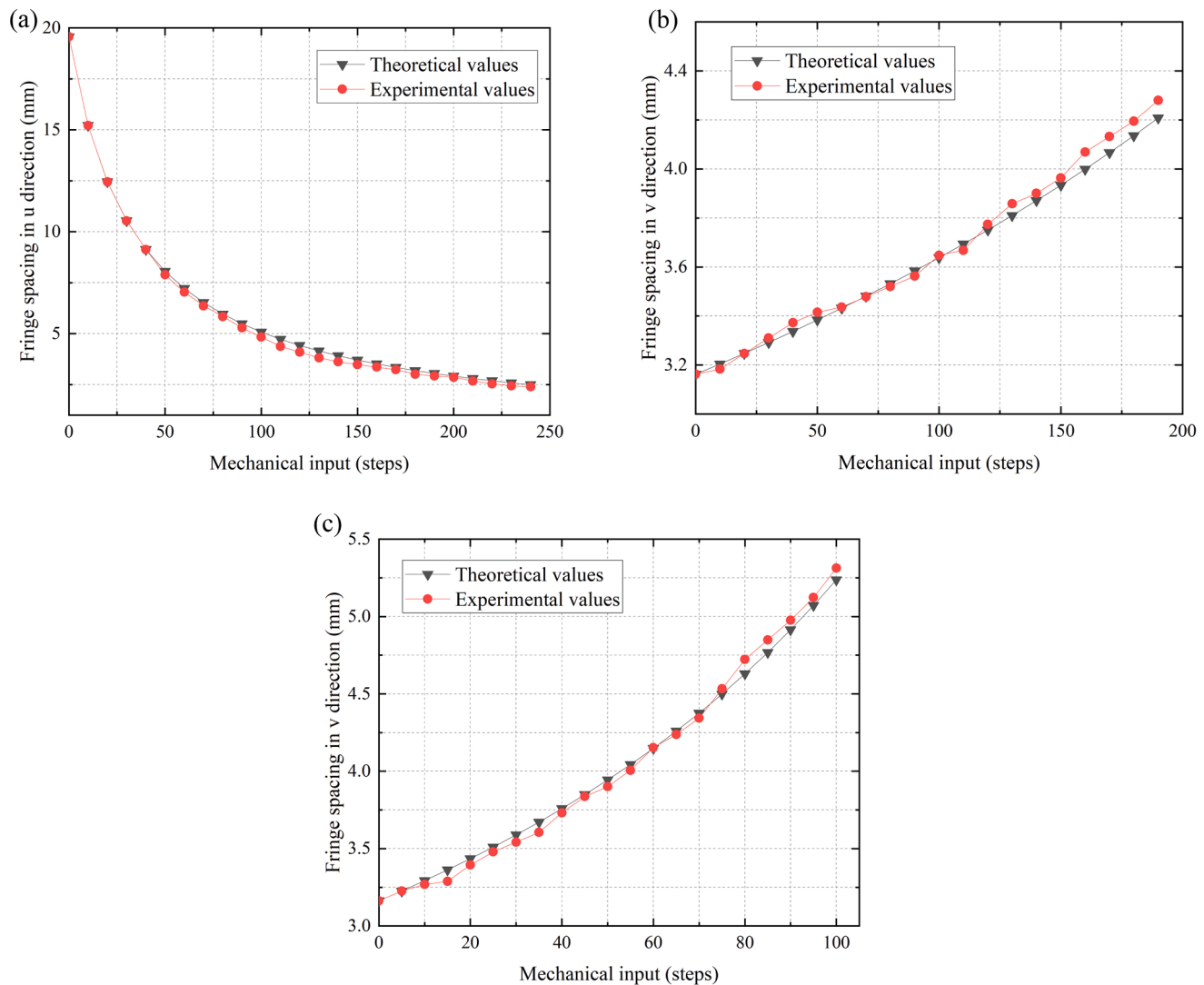


Fig. 7. Theoretical and experimental values of fringe pattern variations with deliberately introduced angular errors (a) $\Delta\theta_y$, mechanical input 10 steps ($4.29 \mu\text{rad}$) each time, (b) $\Delta\theta_x$, mechanical input 10 steps ($3 \mu\text{rad}$) each time, (c) $\Delta\theta_z$, mechanical input 5 steps ($2.15 \mu\text{rad}$) each time.

Comparison of fringe spacing stepping change in u direction caused by $\Delta\theta_y$ is shown in Fig. 7(a). The experimental results were calculated using fringe slope as the intermediate variable. Fig. 7(b)&(c) are tests about fringe spacing stepping change in v direction caused by $\Delta\theta_x$ and $\Delta\theta_z$ respectively. Differences between theoretical and experimental values were lesser than $1/20$ of the fringe spacing. Therefore we can derive that angular alignment sensitivity was better than 1 arcsec. For shifts along x axis and z axis which are controlled by PZTs, the mechanical accuracy (0.2 nm) is above our designed request. Measurement results are more restricted by the resolving power of fringes. For our setup, the fringe spacing was around 150 pixels. According to Eq. (7c), a translation of 725.3 nm along x axis or 351.6 nm along z axis would cause a 2π phase shift in the -36 th order, and the values for the -37 th order are 831.8 nm and 342.1 nm. This means the minimum resolution requirement is estimated 5.5 nm/pixel. Considering marking errors in the process, a translation sensitivity of 10 nm could be achieved conservatively. In addition, fringes were slightly distorted due to aberration. It was mostly produced by deviation of the commercially purchased shearing plate. This error as well as other minor set-up errors in the light path affected simultaneously on both gratings. Since we are resolving relative errors between two gratings, they should have limited influence on the final result.

5. Conclusion

In this paper, we proposed a simple method for gratings tiling based on lateral shearing interferometry specifically designed for echelles. Theoretical analysis has proved the necessity of doing measurements from two different diffraction orders. Mathematical relation between mosaic errors and fringe patterns was investigated and simulated. A verification experiment was demonstrated using a customized mosaic mechanism. Angular and translation sensitivities of 1 arcsec and 10 nm were achieved. More precise optical and mechanical components could further improve measurement accuracy.

CRedit authorship contribution statement

Yifan Li: Data curation, Formal analysis, Investigation, Methodology, Writing – original draft. **Xiaotao Mi:** Data curation, Resources, Writing – review & editing. **Xiangdong Qi:** Conceptualization, Supervision. **Shanwen Zhang:** Conceptualization. **Guojun Yang:** Methodology. **Hongzhu Yu:** Methodology. **Xiaotian Li:** Resources, Funding acquisition. **Wenhao Li:** Supervision.

Declaration of Competing Interest

The authors declare that they have no known competing financial interests or personal relationships that could have appeared to influence the work reported in this paper.

Acknowledgements

The authors acknowledge supports from National Natural Science Foundation of China (62005273, 61975255, 61505204, U2006209); Ministry of Science and Technology of the People's Republic of China (2016YFF0102006, 2016YFF0103304).

References

- [1] V. Mazzacurati, G. Ruocco, The super-gratings - how to improve the limiting resolution of grating spectrometers, *Opt. Commun.* 76 (3–4) (1990) 185–190, [https://doi.org/10.1016/0030-4018\(90\)90279-3](https://doi.org/10.1016/0030-4018(90)90279-3).
- [2] T. Blasiak, S. Zheleznyak, History and construction of large mosaic diffraction gratings, in: A.M. Larar, M.G. Mlynczak (Eds.), *Optical Spectroscopic Techniques, Remote Sensing, and Instrumentation for Atmospheric and Space Research IV*, vol. 4485, International Society for Optics and Photonics; SPIE, 2002, pp. 370–377. doi: 10.1117/12.454272.
- [3] T.J. Zhang, M. Yonemura, Y. Kato, An array-grating compressor for high-power chirped-pulse amplification lasers, *Opt. Commun.* 145 (1–6) (1998) 367–376, [https://doi.org/10.1016/S0030-4018\(97\)00356-8](https://doi.org/10.1016/S0030-4018(97)00356-8).
- [4] T.J. Kessler, J. Bunkenburg, H. Huang, A. Kozlov, D.D. Meyerhofer, Demonstration of coherent addition of multiple gratings for high-energy chirped-pulse-amplified lasers, *Opt. Lett.* 29 (6) (2004) 635–637, <https://doi.org/10.1364/OL.29.000635>.
- [5] J. Bunkenburg, T.J. Kessler, W. Skulski, H. Huang, Phase-locked control of tiled-grating assemblies for chirped-pulse-amplified lasers using a mach-zehnder interferometer, *Opt. Lett.* 31 (10) (2006) 1561–1563, <https://doi.org/10.1364/OL.31.001561>.
- [6] T. Harimoto, Far-field pattern analysis for an array grating compressor, *Jpn. J. Appl. Phys.* 43 (4A) (2004) 1362–1365, <https://doi.org/10.1143/jjap.43.1362>.
- [7] J. Qiao, A. Kalb, M.J. Guardalben, G.D. King, Large-aperture grating tiling by interferometry for petawatt chirped-pulse-amplification systems, *Opt. Express* 15 (15) (2007) 9562–9574.
- [8] L.J. Zeng, L.F. Li, Method of making mosaic gratings by using a two-color heterodyne interferometer containing a reference grating, *Opt. Lett.* 31 (2) (2006) 152–154, <https://doi.org/10.1364/ol.31.000152>.
- [9] A.K. Sharma, A.S. Joshi, P.A. Naik, P.D. Gupta, Active phase locking of a tiled two-grating assembly for high-energy laser pulse compression using simultaneous controls from far-field profiles and interferometry, *Appl. Phys. B* 123 (4) (2017) 117, <https://doi.org/10.1007/s00340-017-6682-2>.
- [10] Y.X. Lu, X.D. Qi, X.T. Li, H.L. Yu, S. Jiang, H. Bayan, L. Yin, Removal of all mosaic grating errors in a single-interferometer system by a phase-difference reference window, *Appl. Opt.* 55 (28) (2016) 7997–8002, <https://doi.org/10.1364/ao.55.007997>.
- [11] J.L. Lizon, H. Dekker, A. Manescau, D. Megevan, F.A. Pepe, M. Riva, A large mosaic echelle grating for ESPRESSO spectrograph, in: M.J. Creech-Eakman, P.G. Tuthill, A. Mérand (Eds.), *Optical and Infrared Interferometry and Imaging VI*, vol. 10701, International Society for Optics and Photonics; SPIE, 2018, pp. 766–775. doi: 10.1117/12.2312435.
- [12] M. Cong, X.D. Qi, X.T. Mi, H.S. Bayan, Interference method for mosaicking echelles using double-angle incident light and a mirror-echelle structure, *Opt. Eng.* 57 (6) (2018), <https://doi.org/10.1117/1.Oe.57.6.064111>.
- [13] A. Cotel, M. Castaing, P. Pichon, C. Le Blanc, Phased-array grating compression for high-energy chirped pulse amplification lasers, *Opt. Express* 15 (5) (2007) 2742–2752, <https://doi.org/10.1364/oe.15.002742>.
- [14] Y. Hu, L. Zeng, Grating mosaic based on image processing of far-field diffraction intensity patterns in two wavelengths, *Appl. Opt.* 46 (28) (2007) 7018–7025, <https://doi.org/10.1364/AO.46.007018>.
- [15] G. Yang, X. Qi, X. Mi, S. Zhang, H. Yu, H. Yu, X. Li, Separation detection and correction of mosaic errors in mosaic gratings based on two detection lights with the same diffraction order and different incident angles, *Opt. Lasers Eng.* 139 (2021) 106281, <https://doi.org/10.1016/j.optlaseng.2020.106281>.
- [16] Y. Hu, W. Wang, Lateral shearing interferometry applied for phase measurement in wavefront coherent synthesis, in: X. Lin, Y. Namba, T. Xing (Eds.), 6th International Symposium on Advanced Optical Manufacturing and Testing Technologies: Optical System Technologies for Manufacturing and Testing, vol. 8420, International Society for Optics and Photonics; SPIE, 2012, pp. 208–213. doi: 10.1117/12.974986.
- [17] D. Daiya, R. Patidar, A. Moorti, N. Benerji, A. Joshi, Simple wedge plate based lateral shearing interferometry technique for coherent alignment of tiled grating assembly, *Opt. Commun.* 459 (2020) 125067, <https://doi.org/10.1016/j.optcom.2019.125067>.
- [18] M.E. Riley, M.A. Gusinow, Laser beam divergence utilizing a lateral shearing interferometer, *Appl. Opt.* 16 (10) (1977) 2753–2756.